

ORBGRAND: Achievable Rate for General Bit Channels and Application in BICM

Zhuang Li and Wenyi Zhang

Department of Electronic Engineering and Information Science

University of Science and Technology of China

Hefei, China

Email: lizhuang06@mail.ustc.edu.cn, wenyizha@ustc.edu.cn

Abstract—Guessing random additive noise decoding (GRAND) has received widespread attention recently, and among its variants, ordered reliability bits GRAND (ORBGRAND) is particularly attractive due to its efficient utilization of soft information and its amenability to hardware implementation. It has been recently shown that ORBGRAND is almost capacity-achieving in additive white Gaussian noise channels under antipodal input. In this work, we first extend the analysis of ORBGRAND achievable rate to memoryless binary-input bit channels with general output conditional probability distributions. The analytical result also sheds insight into understanding the gap between the ORBGRAND achievable rate and the channel mutual information. As an application of the analysis, we study the ORBGRAND achievable rate of bit-interleaved coded modulation (BICM). Numerical results indicate that for BICM, the gap between the ORBGRAND achievable rate and the channel mutual information is typically small, and hence suggest the feasibility of ORBGRAND for channels with high-order coded modulation schemes.

Index Terms—Bit channel, bit-interleaved coded modulation, generalized mutual information, guessing random additive noise decoding.

I. INTRODUCTION

Guessing random additive noise decoding (GRAND) [1] [2] has been recently proposed as a universal decoding paradigm. Its basic idea is to sort and test a sequence of possible error patterns until finding a valid codeword. If all error patterns are sorted from the most likely to the least likely, then GRAND is, in fact, equivalent to maximum-likelihood (ML) decoding.

Utilizing soft symbol reliability information can improve decoding performance [3, Ch. 10]. Symbol reliability GRAND (SRGRAND) [4] uses one bit of soft information to specify whether a channel output symbol is reliable. Soft GRAND (SGRAND) [5] uses magnitudes of channel output to generate error patterns, so it can make full usage of channel soft information and it in fact implements the maximum-likelihood decoding. But SGRAND requires a sequential online algorithm to generate the sequence of error patterns, and this limits its efficiency of hardware implementation. Another variant of GRAND, called ordered reliability bits GRAND (ORBGRAND) [6], does not require exact values of channel output, and instead uses only the relationship of ranking among channel outputs to generate error patterns. This property enables

ORBGRAND to generate error patterns offline and facilitates hardware implementation [7] [8] [9]. Noteworthy, it has been shown via an information theoretic analysis in [10] that, ORBGRAND achieves an information rate almost approaching the channel mutual information in additive white Gaussian noise (AWGN) channels under antipodal input.

Several variants of GRAND have been proposed for fading channels. In [11], ORBGRAND based on reduced-complexity pseudo-soft information has been studied. In [12], fading-GRAND has been proposed for Rayleigh fading channels, shown to outperform traditional hard-decision decoders, and in [13], a hardware architecture of fading-GRAND has been studied. In [14], symbol-level GRAND has been proposed for block fading channels, utilizing the knowledge of modulation scheme and channel state information (CSI). In [15] [16], GRAND has been applied to multiple-input-multiple-output channels.

In this paper, along the line of [10], we conduct an information theoretic analysis to study the performance limit of ORBGRAND, for general memoryless binary-input bit channels. The motivation is that, achievable rates for general bit channels serve as basic building blocks for assessing the performance of ORBGRAND for channels with high-order coded modulation schemes, such as bit-interleaved coded modulation (BICM) [17] [18], a technique extensively used in fading channels. Since ORBGRAND is a mismatched decoding method, rather than the maximum-likelihood one, we utilize generalized mutual information (GMI) to quantify its achievable rate [19] [20]. A comparison between the derived GMI of ORBGRAND and the channel mutual information also sheds insight into understanding the gap between them, helping explain when and why the GMI of ORBGRAND is close to the channel mutual information, as usually observed in numerical studies. As an application of the analysis, we study the ORBGRAND achievable rate of BICM. Numerical results for QPSK, 8PSK, and 16QAM with Gray and set-partitioning labelings over AWGN and Rayleigh fading channels are presented. These results indicate that for BICM, the gap between the ORBGRAND achievable rate and the channel mutual information is typically small, and hence suggest the feasibility of ORBGRAND for channels with high-order coded modulation schemes.

This work was supported in part by the National Natural Science Foundation of China under Grant 62231022.

The remaining part of this paper is organized as follows: Section II introduces the system model and ORBGRAND for general memoryless binary-input bit channels. Section III derives the GMI of ORBGRAND and discusses the gap between it and the channel mutual information. Section IV presents the corresponding numerical results for BICM. Section V concludes this paper.

II. SYSTEM MODEL AND ORBGRAND FOR GENERAL BIT CHANNELS

A. System Model

In this paper, we study memoryless binary-input channels with general output conditional probability distributions. Without loss of generality, let the input alphabet be $\{+1, -1\}$, and let the output probability distribution be $q_+(y)$ under input $x = +1$ and $q_-(y)$ under input $x = -1$, respectively. Note that $q_+(y)$ and $q_-(y)$ are general and we do not require them to possess any symmetric property.

We consider a codebook with code length N and code rate R nats per channel use, so the number of messages is $M = \lceil e^{NR} \rceil$. When sending message m , the transmitted codeword is $\underline{x}(m) = [x_1(m), x_2(m), \dots, x_N(m)]$. We assume that the elements of $\underline{x}(m)$ are independent and identically distributed (i.i.d.) uniform $\{+1, -1\}$ random variables. This is a common assumption in random coding analysis, and is satisfied for many linear codes. The channel output vector is denoted as $\underline{Y} = [Y_1, Y_2, \dots, Y_N]$. Define the log-likelihood ratio (LLR) random variable $T_n = \ln \frac{q_+(Y_n)}{q_-(Y_n)}$ and the reliability vector $[|T_1|, |T_2|, \dots, |T_N|]$. For $n = 1, 2, \dots, N$, denote R_n as the rank of $|T_n|$ among the sorted array consisting of $\{|T_1|, |T_2|, \dots, |T_N|\}$, from 1 (the smallest) to N (the largest). The cumulative distribution function (cdf) of $|T|$ is denoted as $\Psi(t)$, for $t \geq 0$. We use lowercase letters to denote the realizations of random variables; for example, r_n as the realization of R_n , and so on.

B. ORBGRAND for General Bit Channels

For a general bit channel, the procedure of ORBGRAND can be described as follows: when a channel output vector \underline{y} is received, we calculate its reliability vector $[|t_1|, |t_2|, \dots, |t_N|]$ and its hard-decision vector $\underline{x}_{\text{hard}} = [\text{sgn}(t_1), \text{sgn}(t_2), \dots, \text{sgn}(t_N)]$, where $t_i = \ln \frac{q_+(y_i)}{q_-(y_i)}$ is the LLR and $\text{sgn}(t) = 1$ if $t \geq 0$ and -1 otherwise. We generate an error pattern matrix P of size $2^N \times N$. The elements of P are $+1$ or -1 , and the rows of P are all distinct: if the q -th row n -th column element $P_{q,n}$ is -1 , then in the q -th query, we flip the sign of the n -th element of $\underline{x}_{\text{hard}}$. So each row of P represents a different query and we conduct the queries from top to bottom, until finding a valid codeword and declaring it as the decoded codeword, or exhausting all the rows without finding a valid codeword and declaring a decoding failure. We arrange the rows of P so that the sum reliability of the q -th row defined as $\sum_{n: P_{q,n}=-1} r_n$ is non-decreasing with q , where r_n is the rank of $|t_n|$ introduced in the previous subsection. There exist efficient algorithms for generating the matrix P ; see, e.g., [6] [7]. Since 2^N is typically an exceedingly large

quantity, in practice we can truncate the matrix to keep only its first Q rows, where Q is the maximum number of queries permitted.

As shown in [10], the following form of decoding criterion provides a unified description of GRAND and its variants including ORBGRAND, if Q is set to its maximum possible value 2^N : for a received channel output vector \underline{y} , the decoder decides the message to be

$$\hat{m} = \arg \min_{m=1,2,\dots,M} \frac{1}{N} \sum_{n=1}^N \gamma_n(\underline{y}) \cdot \mathbf{1} \left(\text{sgn} \left(\ln \frac{q_+(y_n)}{q_-(y_n)} \right) \cdot x_n(m) < 0 \right). \quad (1)$$

It can be shown (for details see, e.g., [10, Sec. II]) that the decoding criterion (1) produces the same decoding result as, and is hence equivalent to, GRAND and its variants, if we are permitted to conduct an exhaustive query of all possible error patterns, i.e., $Q = 2^N$.¹ Different choices of $\{\gamma_n\}_{n=1,2,\dots,N}$ correspond to different sorting criteria of error patterns: if $\gamma_n(\underline{y}) = 1$, (1) is the original GRAND [1]; if $\gamma_n(\underline{y}) = \left\lfloor \ln \frac{q_+(y_n)}{q_-(y_n)} \right\rfloor$, (1) is SGRAND [5], which is equivalent to the maximum-likelihood decoding; if $\gamma_n(\underline{y}) = \frac{r_n}{N}$, where r_n is the realization of the rank random variable R_n , (1) is ORBGRAND [6].

III. GMI ANALYSIS OF ORBGRAND

A. GMI of ORBGRAND

Since ORBGRAND is not the maximum likelihood decoding, we resort to mismatched decoding analysis (see, e.g., [19] [20]) for characterizing its information theoretic performance limit. For this purpose, GMI is a convenient tool and has been widely used. GMI quantifies the maximum rate such that the ensemble average probability of decoding error asymptotically vanishes as the code length grows without bound. For general memoryless bit channels, the GMI of ORBGRAND is characterized by the following theorem.

Theorem 1: For the system setup in Section II, the GMI of ORBGRAND is given by

$$I_{\text{ORBGRAND}} = \ln 2 - \inf_{\theta < 0} \left\{ \int_0^1 \ln(1 + e^{\theta t}) dt - \theta \cdot \frac{1}{2} \int_{q_+(y) < q_-(y)} \Psi \left(\left| \ln \frac{q_+(y)}{q_-(y)} \right| \right) q_+(y) dy - \theta \cdot \frac{1}{2} \int_{q_+(y) > q_-(y)} \Psi \left(\left| \ln \frac{q_+(y)}{q_-(y)} \right| \right) q_-(y) dy \right\} \quad (2)$$

in nats/channel use.

Proof: Since in ORBGRAND, the terms inside the summation in (1) are correlated due to the relationship of ranking, we cannot directly invoke the standard formula of GMI (see,

¹As mentioned in the previous paragraph, in practice Q is usually set as a number smaller than 2^N , but the form of (1) renders an information theoretic analysis amenable, as will be seen in the next section.

e.g., [19, Eqn. (12)]) to evaluate the GMI of ORBGRAND. Instead, we conduct analysis and calculation from the first principle, similar to [10] which considers the special case of AWGN channels only. We calculate the ensemble average probability of decoding error. As a consequence of i.i.d. random coding, the average probability of decoding error is equal to the probability of decoding error under the condition of transmitting message $m = 1$.

Based on the general decoding rule (1), we define the decoding metric of ORBGRAND by

$$D(m) = \frac{1}{N} \sum_{n=1}^N \frac{R_n}{N} \cdot \mathbf{1}(\text{sgn}(\mathbf{T}_n) \cdot \mathbf{X}_n(m) < 0), \quad m = 1, 2, \dots, M. \quad (3)$$

Under i.i.d random coding, $\{\mathbf{T}_n\}_{n=1,2,\dots,N}$ are also i.i.d. with cdf $\Psi(t)$, for $t \geq 0$.

When the transmitted message is $m = 1$, we can characterize the asymptotic behavior of the decoding metric in (3) using the following three lemmas, whose proofs are placed in Appendix A.

Lemma 1: As $N \rightarrow \infty$, for the transmitted codeword, the expectation of the decoding metric in (3) is given by

$$\lim_{N \rightarrow +\infty} \mathbb{E}D(1) = \frac{1}{2} \int_{q_+(y) < q_-(y)} \Psi\left(\left|\ln \frac{q_+(y)}{q_-(y)}\right|\right) q_+(y) dy + \frac{1}{2} \int_{q_+(y) > q_-(y)} \Psi\left(\left|\ln \frac{q_+(y)}{q_-(y)}\right|\right) q_-(y) dy. \quad (4)$$

Lemma 2: As $N \rightarrow \infty$, for the transmitted codeword, the variance of the decoding metric in (3) is given by

$$\lim_{N \rightarrow +\infty} \text{var}D(1) = 0. \quad (5)$$

Lemma 3: As $N \rightarrow \infty$, for any codeword not transmitted, i.e., $m' \neq 1$ and any $\theta < 0$, the decoding metric in (3) satisfies, almost surely,

$$\Delta(\theta) := \lim_{N \rightarrow +\infty} \frac{1}{N} \ln \mathbb{E} \left\{ e^{N\theta D(m')} \middle| \mathbf{T} \right\} = \int_0^1 \ln(1 + e^{\theta t}) dt - \ln 2. \quad (6)$$

For any $\epsilon > 0$, we define event

$$\mathcal{U}_\epsilon = \left\{ D(1) \geq \frac{1}{2} \int_{q_+(y) < q_-(y)} \Psi\left(\left|\ln \frac{q_+(y)}{q_-(y)}\right|\right) q_+(y) dy + \frac{1}{2} \int_{q_+(y) > q_-(y)} \Psi\left(\left|\ln \frac{q_+(y)}{q_-(y)}\right|\right) q_-(y) dy + \epsilon \right\},$$

so the ensemble average probability of decoding error is

$$\begin{aligned} & \Pr[\hat{m} \neq 1] \\ &= \Pr[\hat{m} \neq 1 | \mathcal{U}_\epsilon] \Pr[\mathcal{U}_\epsilon] + \Pr[\hat{m} \neq 1 | \mathcal{U}_\epsilon^c] \Pr[\mathcal{U}_\epsilon^c] \\ &\leq \Pr[\mathcal{U}_\epsilon] + \Pr[\hat{m} \neq 1 | \mathcal{U}_\epsilon^c]. \end{aligned} \quad (7)$$

Using Lemma 1, Lemma 2 and Chebyshev's inequality, we can deduce that for any $\epsilon > 0$,

$$\begin{aligned} \lim_{N \rightarrow +\infty} \Pr \left[D(1) \geq \frac{1}{2} \int_{q_+(y) < q_-(y)} \Psi\left(\left|\ln \frac{q_+(y)}{q_-(y)}\right|\right) q_+(y) dy \right. \\ \left. + \frac{1}{2} \int_{q_+(y) > q_-(y)} \Psi\left(\left|\ln \frac{q_+(y)}{q_-(y)}\right|\right) q_-(y) dy + \epsilon \right] = 0; \end{aligned} \quad (8)$$

this shows that $\Pr[\mathcal{U}_\epsilon]$ can be arbitrarily close to zero as the code length N grows without bound.

Meanwhile, based on the decoding rule (1) and the union bound, we have

$$\begin{aligned} & \Pr[\hat{m} \neq 1 | \mathcal{U}_\epsilon^c] \\ &\leq \Pr \left[\exists m' \neq 1, D(m') < \frac{1}{2} \int_{q_+(y) < q_-(y)} \Psi\left(\left|\ln \frac{q_+(y)}{q_-(y)}\right|\right) q_+(y) dy \right. \\ &\quad \left. + \frac{1}{2} \int_{q_+(y) > q_-(y)} \Psi\left(\left|\ln \frac{q_+(y)}{q_-(y)}\right|\right) q_-(y) dy + \epsilon \right] \\ &\leq e^{NR} \Pr \left[D(m') < \frac{1}{2} \int_{q_+(y) < q_-(y)} \Psi\left(\left|\ln \frac{q_+(y)}{q_-(y)}\right|\right) q_+(y) dy \right. \\ &\quad \left. + \frac{1}{2} \int_{q_+(y) > q_-(y)} \Psi\left(\left|\ln \frac{q_+(y)}{q_-(y)}\right|\right) q_-(y) dy + \epsilon \right]. \end{aligned} \quad (9)$$

Considering the conditional version of the probability in (9), and applying Chernoff's bound, we have that for any N and any $\theta < 0$,

$$\begin{aligned} & -\frac{1}{N} \ln \Pr \left[D(m') < \frac{1}{2} \int_{q_+(y) < q_-(y)} \Psi\left(\left|\ln \frac{q_+(y)}{q_-(y)}\right|\right) q_+(y) dy \right. \\ &\quad \left. + \frac{1}{2} \int_{q_+(y) > q_-(y)} \Psi\left(\left|\ln \frac{q_+(y)}{q_-(y)}\right|\right) q_-(y) dy + \epsilon \middle| \mathbf{T} \right] \\ &\geq \theta \left[\frac{1}{2} \int_{q_+(y) < q_-(y)} \Psi\left(\left|\ln \frac{q_+(y)}{q_-(y)}\right|\right) q_+(y) dy + \frac{1}{2} \int_{q_+(y) > q_-(y)} \Psi\left(\left|\ln \frac{q_+(y)}{q_-(y)}\right|\right) q_-(y) dy + \epsilon \right] \\ &\quad - \frac{1}{N} \ln \mathbb{E} \left\{ e^{N\theta D(m')} \middle| \mathbf{T} \right\}. \end{aligned} \quad (10)$$

Letting $\epsilon \rightarrow 0$, the code length $N \rightarrow +\infty$, and applying the almost surely limit in Lemma 3, we have

$$\begin{aligned} & \Pr \left[D(m') < \frac{1}{2} \int_{q_+(y) < q_-(y)} \Psi\left(\left|\ln \frac{q_+(y)}{q_-(y)}\right|\right) q_+(y) dy \right. \\ &\quad \left. + \frac{1}{2} \int_{q_+(y) > q_-(y)} \Psi\left(\left|\ln \frac{q_+(y)}{q_-(y)}\right|\right) q_-(y) dy + \epsilon \middle| \mathbf{T} \right] \\ &\leq \exp \left\{ -N \left[\theta \cdot \frac{1}{2} \int_{q_+(y) < q_-(y)} \Psi\left(\left|\ln \frac{q_+(y)}{q_-(y)}\right|\right) q_+(y) dy \right. \right. \\ &\quad \left. \left. + \theta \cdot \frac{1}{2} \int_{q_+(y) > q_-(y)} \Psi\left(\left|\ln \frac{q_+(y)}{q_-(y)}\right|\right) q_-(y) dy \right. \right. \\ &\quad \left. \left. - \int_0^1 \ln(1 + e^{\theta t}) dt + \ln 2 \right] \right\}. \end{aligned} \quad (11)$$

Substituting (11) into (9), and applying the law of total expectation to remove the conditioning, we assert that the ensemble average probability of decoding error asymptotically vanishes as the code length N grows without bound if the code rate R satisfies the following inequality, i.e., (2) in the statement of Theorem 1.

$$\begin{aligned}
R &< \sup_{\theta < 0} \left\{ \theta \cdot \frac{1}{2} \int_{q_+(y) < q_-(y)} \Psi \left(\left| \ln \frac{q_+(y)}{q_-(y)} \right| \right) q_+(y) dy \right. \\
&\quad + \theta \cdot \frac{1}{2} \int_{q_+(y) > q_-(y)} \Psi \left(\left| \ln \frac{q_+(y)}{q_-(y)} \right| \right) q_-(y) dy \\
&\quad \left. - \int_0^1 \ln(1 + e^{\theta t}) dt + \ln 2 \right\} \\
&= \ln 2 - \inf_{\theta < 0} \left\{ \int_0^1 \ln(1 + e^{\theta t}) dt \right. \\
&\quad - \theta \cdot \frac{1}{2} \int_{q_+(y) < q_-(y)} \Psi \left(\left| \ln \frac{q_+(y)}{q_-(y)} \right| \right) q_+(y) dy \\
&\quad \left. - \theta \cdot \frac{1}{2} \int_{q_+(y) > q_-(y)} \Psi \left(\left| \ln \frac{q_+(y)}{q_-(y)} \right| \right) q_-(y) dy \right\}.
\end{aligned} \tag{12}$$

□

B. Discussion on Gap between GMI of ORBGRAND and Channel Mutual Information

For general memoryless bit channels under uniform binary input, as described in Section II-A, the channel mutual information is given by

$$\begin{aligned}
I &= I(X; Y) \\
&= \ln 2 - \frac{1}{2} \int_{-\infty}^{+\infty} \ln \left(1 + \frac{q_-(y)}{q_+(y)} \right) q_+(y) dy \\
&\quad - \frac{1}{2} \int_{-\infty}^{+\infty} \ln \left(1 + \frac{q_+(y)}{q_-(y)} \right) q_-(y) dy
\end{aligned} \tag{13}$$

in nats/channel use.

In order to analyze the gap between (2) and (13), we rewrite (13) into its equivalent form as the GMI of SGRAND, noticing that SGRAND is equivalent to the maximum-likelihood decoding and thus achieves the channel mutual information. This leads to the following result.

Proposition 1: For the general memoryless bit channel model in Section II, the GMI of SGRAND is given by

$$\begin{aligned}
I_{\text{SGRAND}} &= \ln 2 - \inf_{\theta < 0} \left\{ \mathbb{E} \left[\ln \left(1 + e^{\theta \left| \ln \frac{q_+(Y)}{q_-(Y)} \right|} \right) \right] \right. \\
&\quad - \theta \cdot \frac{1}{2} \int_{q_+(y) < q_-(y)} \left| \ln \frac{q_+(y)}{q_-(y)} \right| q_+(y) dy \\
&\quad \left. - \theta \cdot \frac{1}{2} \int_{q_+(y) > q_-(y)} \left| \ln \frac{q_+(y)}{q_-(y)} \right| q_-(y) dy \right\}
\end{aligned} \tag{14}$$

in nats/channel use, and this is equal to the channel mutual information I in (13).

Proof: See Appendix B.

□

It is interesting to note that, if $\left| \ln \frac{q_+(Y)}{q_-(Y)} \right|$ and $\left| \ln \frac{q_-(Y)}{q_+(Y)} \right|$ in (14) are replaced by $\Psi \left(\left| \ln \frac{q_+(Y)}{q_-(Y)} \right| \right)$ and $\Psi \left(\left| \ln \frac{q_-(Y)}{q_+(Y)} \right| \right)$ respectively, then (14) will become (2). This is obtained by noting that $\Psi \left(\left| \ln \frac{q_+(Y)}{q_-(Y)} \right| \right)$ obeys the uniform distribution over $[0, 1]$ and hence

$$\mathbb{E} \left[\ln \left(1 + e^{\theta \Psi \left(\left| \ln \frac{q_+(Y)}{q_-(Y)} \right| \right)} \right) \right] = \int_0^1 \ln(1 + e^{\theta t}) dt. \tag{15}$$

Therefore, the gap between I_{ORBGRAND} and I is essentially caused by the difference between t and $\Psi(t)$. If $\Psi(t)$ behaves close to a linear function, then the GMI of ORBGRAND will be close to the channel mutual information.

Here we give a simple example to illustrate the above discussion. We consider BPSK modulation over the Rayleigh fading channel with perfect CSI and the AWGN channel. The curves of $\Psi(t)$ and I_{ORBGRAND} under different values of signal-to-noise ratio (SNR) are displayed in Fig. 1 and Fig. 2, respectively. Taking SNR = 3dB as an example, we can see from Fig. 1 that the linearity of $\Psi(t)$ in the Rayleigh fading channel is obviously worse than that in the AWGN channel. Therefore, we can see from Fig. 2 that there is a noticeable gap between I_{ORBGRAND} and I in the Rayleigh fading channel, while there is virtually no gap in the AWGN channel.

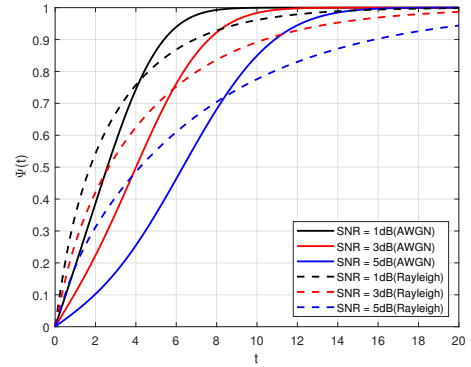


Fig. 1. Plots of $\Psi(t)$ under under AWGN and Rayleigh fading channels.

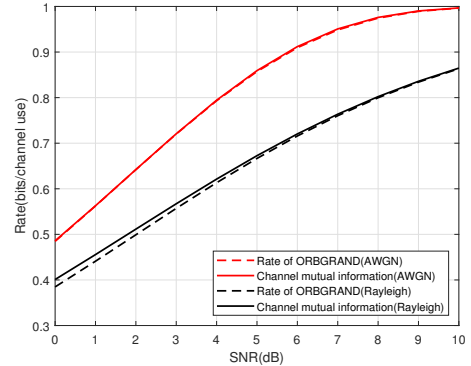


Fig. 2. Plots of I_{ORBGRAND} and I under AWGN and Rayleigh fading channels.

IV. APPLICATION IN BICM

BICM is an effective coded modulation scheme and has been widely used in contemporary communication systems. In this section, we use the analytical results in the previous section to calculate the ORBGRAND achievable rate of BICM, and compare it with the channel mutual information. This study serves as a theoretical basis for the feasibility of ORBGRAND for channels with high-order coded modulation schemes.

A. Experimental Setup

In our experiment, we consider QPSK, 8PSK and 16QAM with ideal interleaving and perfect CSI. For each modulation type, we consider both Gray and set-partitioning labelings. For example, the constellation diagrams of the two labelings for 16QAM are shown in Fig. 3. The channel input-output relationship is

$$Y = HS + Z. \quad (16)$$

H is the channel gain: when $H = 1$, (16) is the AWGN channel, and when H obeys a unit-variance circularly symmetric complex Gaussian distribution, (16) is the Rayleigh fading channel; S is the channel input, corresponding to a point in the constellation diagram; Z is the standard circularly symmetric complex Gaussian noise. In BICM, the codeword \mathbf{X} is first passed to an interleaver π , and the interleaved sequence $\pi(\mathbf{X})$ is then divided into multiple subsequences, each of length matched to the order of the constellation, and is thus mapped to a point in the constellation diagram according to a certain labeling rule; for details, see, e.g., [17] [18].

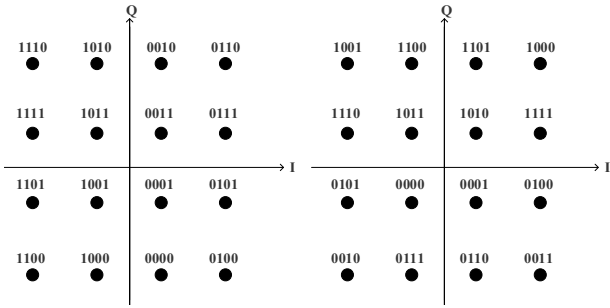


Fig. 3. Gray (left) and set-partitioning (right) labelings for 16QAM.

Due to the nature of ideal interleaving, we can adopt the concept of parallel channel model in [17], as shown in Fig. 4. The ORBGRAND achievable rate of the i -th parallel channel is denoted as I_{ORBGRAND}^i , so $I_{\text{ORBGRAND}} = \sum_{i=1}^m I_{\text{ORBGRAND}}^i$, where m is the number of parallel channels. For the i -th parallel channel, the conditional probability distribution of y is given by

$$q_+^i(y) = \frac{\sum_{s \in \mathcal{X}_1^i} p(y|s)}{|\mathcal{X}_1^i|}, \quad q_-^i(y) = \frac{\sum_{s \in \mathcal{X}_0^i} p(y|s)}{|\mathcal{X}_0^i|}, \quad (17)$$

where \mathcal{X}_1^i is the set of s whose i -th bit is 1, and \mathcal{X}_0^i is the set of s whose i -th bit is 0. ² Plugging (16) and (17) into (2), we can calculate I_{ORBGRAND}^i , and thus get I_{ORBGRAND} .

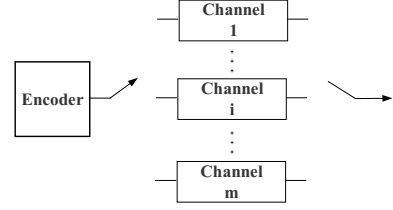


Fig. 4. Parallel channel model of BICM with ideal interleaving.

B. Numerical Results

In general, the ORBGRAND achievable rate and the channel mutual information in BICM do not yield closed-form expressions, so we use numerical methods such as Monte Carlo to evaluate them.

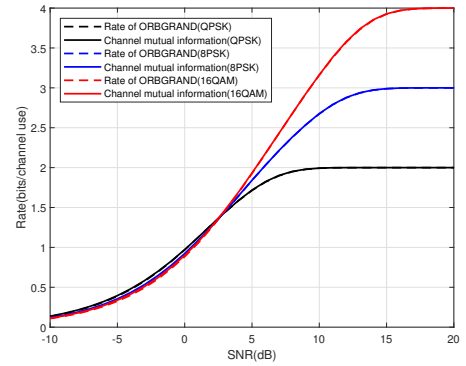


Fig. 5. ORBGRAND achievable rate and channel mutual information under QPSK, 8PSK and 16QAM for AWGN channel in the case of Gray labeling.

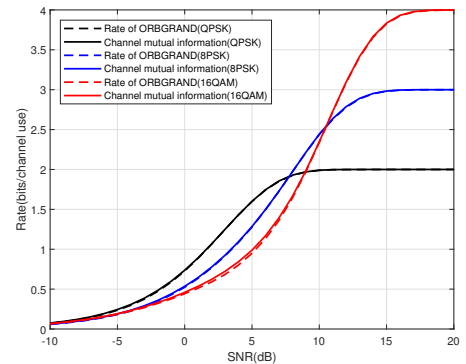


Fig. 6. ORBGRAND achievable rate and channel mutual information under QPSK, 8PSK and 16QAM for AWGN channel in the case of set-partitioning labeling.

²Here, 1 (resp. 0) corresponds to +1 (resp. -1) in our bit channel model in Sections II and III.

The numerical results for the AWGN channel are shown in Fig. 5 and Fig. 6, which show that although ORBGRAND is a mismatched decoder, the ORBGRAND achievable rate under QPSK, 8PSK and 16QAM over the AWGN channel is very close to the channel mutual information, regardless of the labeling. The numerical results for the Rayleigh fading channel are shown in Fig. 7 and Fig. 8, which exhibit essentially the same trend as that in the AWGN channel, with a slightly larger gap between the ORBGRAND achievable rate and the channel mutual information in the low SNR regime. As discussed in Section III-B, the gap is due to the nonlinearity of the cdf of the magnitude of the channel LLR. These numerical results suggest that ORBGRAND can still maintain good decoding performance for channels adopting high-order coded modulation schemes.

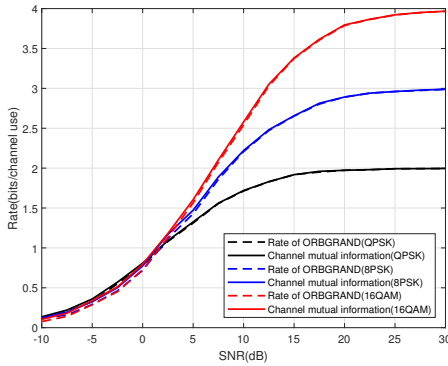


Fig. 7. ORBGRAND achievable rate and channel mutual information under QPSK, 8PSK and 16QAM for Rayleigh fading channel with perfect CSI in the case of Gray labeling.

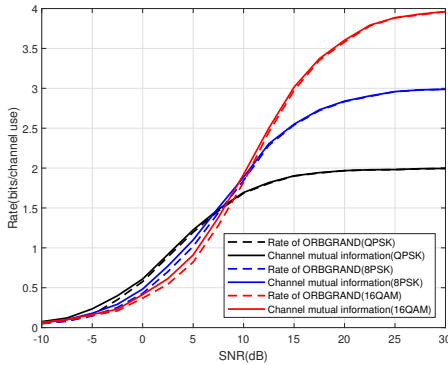


Fig. 8. ORBGRAND achievable rate and channel mutual information under QPSK, 8PSK and 16QAM for Rayleigh fading channel with perfect CSI in the case of set-partitioning labeling.

V. CONCLUSION

In this paper, we conduct an achievable rate analysis of ORBGRAND for memoryless binary-input channels with general output conditional probability distributions. The achievable rate is characterized by the GMI of ORBGRAND, and its

analysis sheds insight into why and when the GMI is close to the channel mutual information, a phenomenon usually observed in several representative channels of practical interest. This analysis further paves the way towards analyzing the performance of ORBGRAND for high-order coded modulation schemes, such as BICM. Numerical results for BICM indicate the near-optimal performance of ORBGRAND, and thus suggest its feasibility for high-rate transmission systems, where high-order modulations are necessary.

APPENDIX A

PROOF OF LEMMAS 1-3

A. Proof of Lemma 1

We have

$$\mathbb{E}D(1) = \frac{1}{N^2} \sum_{n=1}^N \mathbb{E}[R_n \mathbf{1}(\text{sgn}(T_n) \cdot X_n(1) < 0)]. \quad (18)$$

For each term in (18), we have

$$\begin{aligned} & \mathbb{E}[R_n \mathbf{1}(\text{sgn}(T_n) \cdot X_n(1) < 0)] \\ &= \frac{1}{2} \mathbb{E}[R_n \mathbf{1}(T_n < 0) | X_n(1) = +1] \\ & \quad + \frac{1}{2} \mathbb{E}[R_n \mathbf{1}(T_n > 0) | X_n(1) = -1]. \end{aligned} \quad (19)$$

For the first expectation in (19), based on the law of total expectation, we have

$$\begin{aligned} & \mathbb{E}[R_n \mathbf{1}(T_n < 0) | X_n(1) = +1] \\ &= \mathbb{E}\left[\mathbb{E}[R_n \mathbf{1}(q_+(Y_n) < q_-(Y_n)) | X_n(1) = +1, Y_n]\right]. \end{aligned} \quad (20)$$

Next we have

$$\begin{aligned} & \mathbb{E}[R_n \mathbf{1}(q_+(Y_n) < q_-(Y_n)) | X_n(1) = +1, Y_n = y] \\ &= \begin{cases} \mathbb{E}[R_n | X_n(1) = +1, Y_n = y] & \text{if } q_+(y) < q_-(y), \\ 0 & \text{else.} \end{cases} \end{aligned} \quad (21)$$

Based on the definition of R_n and the i.i.d. nature of $\{|T_n|\}_{n=1,2,\dots,N}$, we notice that the expectation in the first branch of (21) is exactly the expectation of the rank when inserting $\left\lfloor \ln \frac{q_+(y)}{q_-(y)} \right\rfloor$ into a sorted array of $N-1$ samples of $\{|T|\}$. For simplicity, denoting the expectation in the first branch of (20) as $u(y)$, so

$$\mathbb{E}[R_n \mathbf{1}(T_n < 0) | X_n(1) = +1] = \int_{q_+(y) < q_-(y)} u(y) q_+(y) dy. \quad (22)$$

The second expectation in (19) can be treated in the same approach. Therefore, we have

$$\begin{aligned} \mathbb{E}D(1) &= \frac{1}{2} \int_{q_+(y) < q_-(y)} \frac{u(y)}{N} q_+(y) dy \\ & \quad + \frac{1}{2} \int_{q_+(y) > q_-(y)} \frac{u(y)}{N} q_-(y) dy. \end{aligned} \quad (23)$$

Utilizing the asymptotic behavior of binomial distribution (for details see [10, Appendix F]), we obtain

$$\lim_{N \rightarrow +\infty} \mathbb{E}D(1) = \frac{1}{2} \int_{q_+(y) < q_-(y)} \Psi \left(\left| \ln \frac{q_+(y)}{q_-(y)} \right| \right) q_+(y) dy + \frac{1}{2} \int_{q_+(y) > q_-(y)} \Psi \left(\left| \ln \frac{q_+(y)}{q_-(y)} \right| \right) q_-(y) dy. \quad (24)$$

B. Proof of Lemma 2

Defining $W_n = \frac{R_n}{N} \mathbf{1}(\text{sgn}(T_n) \cdot X_n(1) < 0)$ and $\tilde{W}_n = W_n - \mathbb{E}W_n$, we have

$$\text{var}D(1) = \frac{1}{N^2} \sum_{i=1}^N \sum_{j=1}^N \mathbb{E}[\tilde{W}_i \tilde{W}_j]. \quad (25)$$

We disassemble (25) into two situations: $j = i$ and $j \neq i$, and then separately treat them following similar techniques as in [10, Appendix C]. The analysis reveals that $\text{var}D(1)$ asymptotically vanishes as $N \rightarrow \infty$.

C. Proof of Lemma 3

Since $\underline{\mathbf{T}}$ is induced by $\underline{\mathbf{X}}(1)$, it is independent of $\underline{\mathbf{X}}(m')$, and we have

$$\mathbb{E} \left\{ e^{N\theta D(m')} \middle| \underline{\mathbf{T}} \right\} = \prod_{n=1}^N \mathbb{E} \left\{ e^{\theta \frac{R_n}{N} \mathbf{1}(\text{sgn}(T_n) \cdot X_n(m') < 0)} \middle| \underline{\mathbf{T}} \right\}. \quad (26)$$

We can use similar approach as in [10, Appendix D], exploiting the fact that R_n is determinisitc once $\underline{\mathbf{T}}$ is given, to obtain

$$\mathbb{E} \left\{ e^{\theta \frac{R_n}{N} \mathbf{1}(\text{sgn}(T_n) \cdot X_n(m') < 0)} \middle| \underline{\mathbf{T}} \right\} = \frac{1}{2} (1 + e^{\theta \frac{R_n}{N}}). \quad (27)$$

Substituting (27) into (26) and using the fact that $\{R_n\}_{n=1,2,\dots,N}$ is a permutation of $\{1, 2, \dots, N\}$, we obtain

$$\Delta(\theta) = \int_0^1 \ln(1 + e^{\theta t}) dt - \ln 2. \quad (28)$$

APPENDIX B

GMI OF SGRAND

The GMI of SGRAND can be calculated by the formula of GMI [19, Eqn. (12)] as

$$I_{\text{SGRAND}} = \sup_{\theta < 0} \left\{ \theta \mathbb{E}d(\mathbf{X}, \mathbf{Y}) - \mathbb{E} \left[\ln \sum_{x \in \{+1, -1\}} \frac{e^{\theta d(x, \mathbf{Y})}}{2} \right] \right\}, \quad (29)$$

where $d(x, y) = \left| \ln \frac{q_+(y)}{q_-(y)} \right| \cdot \mathbf{1} \left(\text{sgn} \left(\ln \frac{q_+(y)}{q_-(y)} \right) \cdot x < 0 \right)$.

With some calculations, we have

$$I_{\text{SGRAND}} = \ln 2 - \inf_{\theta < 0} \left\{ \mathbb{E} \left[\ln \left(1 + e^{\theta \left| \ln \frac{q_+(y)}{q_-(y)} \right|} \right) \right] - \theta \cdot \frac{1}{2} \int_{q_+(y) < q_-(y)} \left| \ln \frac{q_+(y)}{q_-(y)} \right| q_+(y) dy - \theta \cdot \frac{1}{2} \int_{q_+(y) > q_-(y)} \left| \ln \frac{q_+(y)}{q_-(y)} \right| q_-(y) dy \right\}. \quad (30)$$

REFERENCES

- [1] K. R. Duffy, J. Li, and M. Médard, "Capacity-achieving guessing random additive noise decoding," *IEEE Transactions on Information Theory*, vol. 65, no. 7, pp. 4023–4040, 2019.
- [2] A. Riaz, M. Medard, K. R. Duffy, and R. T. Yazicigil, "A universal maximum likelihood GRAND decoder in 40nm CMOS," in *14th International Conference on Communication Systems & NETworks (COMSNETS)*, pp. 421–423, 2022.
- [3] S. Lin and D. J. Costello, "Error control coding, second edition," 2004.
- [4] K. R. Duffy, M. Médard, and W. An, "Guessing random additive noise decoding with symbol reliability information (SRGRAND)," *IEEE Transactions on Communications*, vol. 70, no. 1, pp. 3–18, 2021.
- [5] A. Solomon, K. R. Duffy, and M. Médard, "Soft maximum likelihood decoding using GRAND," in *IEEE International Conference on Communications (ICC)*, pp. 1–6, 2020.
- [6] K. R. Duffy, W. An, and M. Médard, "Ordered reliability bits guessing random additive noise decoding," *IEEE Transactions on Signal Processing*, vol. 70, pp. 4528–4542, 2022.
- [7] C. Condo, V. Bioglio, and I. Land, "High-performance low-complexity error pattern generation for ORBGRAND decoding," in *IEEE Globecom Workshops (GC Wkshps)*, pp. 1–6, 2021.
- [8] S. M. Abbas, T. Tonnellier, F. Ercan, M. Jaleddine, and W. J. Gross, "High-throughput and energy-efficient VLSI architecture for ordered reliability bits GRAND," *IEEE Transactions on Very Large Scale Integration (VLSI) Systems*, vol. 30, no. 6, pp. 681–693, 2022.
- [9] C. Condo, "A fixed latency ORBGRAND decoder architecture with LUT-aided error-pattern scheduling," *IEEE Transactions on Circuits and Systems I: Regular Papers*, vol. 69, no. 5, pp. 2203–2211, 2022.
- [10] M. Liu, Y. Wei, Z. Chen, and W. Zhang, "ORBGRAND is almost capacity-achieving," *IEEE Transactions on Information Theory*, vol. 69, no. 5, pp. 2830–2840, 2022.
- [11] H. Sariyedeen, M. Médard, and K. R. Duffy, "GRAND for fading channels using pseudo-soft information," in *IEEE Global Communications Conference*, pp. 3502–3507, 2022.
- [12] S. M. Abbas, M. Jaleddine, and W. J. Gross, "GRAND for Rayleigh fading channels," in *IEEE Globecom Workshops (GC Wkshps)*, pp. 504–509, 2022.
- [13] S. M. Abbas, M. Jaleddine, and W. J. Gross, "Hardware architecture for fading-GRAND," in *Guessing Random Additive Noise Decoding: A Hardware Perspective*, pp. 125–140, Springer, 2023.
- [14] I. Chatzigeorgiou and F. A. Monteiro, "Symbol-level GRAND for high-order modulation over block fading channels," *IEEE Communications Letters*, vol. 27, no. 2, pp. 447–451, 2022.
- [15] S. Allahkaram, F. A. Monteiro, and I. Chatzigeorgiou, "URLLC with coded massive MIMO via random linear codes and GRAND," in *IEEE 96th Vehicular Technology Conference (VTC2022-Fall)*, pp. 1–5, 2022.
- [16] S. Allahkaram, F. A. Monteiro, and I. Chatzigeorgiou, "Symbol-level noise-guessing decoding with antenna sorting for URLLC massive MIMO," *arXiv preprint arXiv:2305.13113*, 2023.
- [17] G. Caire, G. Taricco, and E. Biglieri, "Bit-interleaved coded modulation," *IEEE Transactions on Information Theory*, vol. 44, no. 3, pp. 927–946, 1998.
- [18] A. G. i Fabregas, A. Martinez, G. Caire, *et al.*, "Bit-interleaved coded modulation," *Foundations and Trends® in Communications and Information Theory*, vol. 5, no. 1–2, pp. 1–153, 2008.
- [19] A. Ganti, A. Lapidoth, and I. E. Telatar, "Mismatched decoding revisited: General alphabets, channels with memory, and the wide-band limit," *IEEE Transactions on Information Theory*, vol. 46, no. 7, pp. 2315–2328, 2000.
- [20] A. Lapidoth and S. Shamai, "Fading channels: how perfect need 'perfect side information' be?," *IEEE Transactions on Information Theory*, vol. 48, no. 5, pp. 1118–1134, 2002.